Satellite Dielectronic spectra created from autoionizing $2lnl'$ and $1s2lnl'$ states with n=4-5

U.I. Safronova, A.A. Vasilyev, and R.K. Smith

Abstract: Relative intensities of dielectronic satellite lines determined by radiative transition probabilities and autoionization rates are calculated for the transitions $2lnl'$ - $1snl'$, $2lnl'$ - $1s2l$ (n=4-5, l=0-3) in He-like ions and for the transitions $1s2lnl'$ - $1s^2nl'$, $1s2lnl'$ - $1s^22l$ (n=4-5, l=0-3) in Li-like ions, for all Z=5-54, using the perturbation theory method (Z-expansion). Relativistic effects are taken into account using the Breit-Pauli operators. The asymptotic dependence on n of the energy matrix is discussed for $2lnl'$ and $1s2lnl'$ autoionizing states. Intermediate coupling coefficients obtained after diagonalization the energy matrices are also studied. It was observed that these coefficients change very sharply with n and Z due to a redistribution of the contributions of relativistic and correlation effects. As a result, all other atomic characteristics (radiative and nonradiative transition rates, branching ratios, and relative intensity factor) display non-monotonic Z- and n- dependencies with maxima and minima.

PACS Nos.:32.80.D, 31.20.G, 31.30.J, 31.50

1. Introduction

Satellites are spectral lines that correspond to the same transitions as resonance lines, but occur in the presence of additional electrons. Thus, satellites to resonance lines of H- and He-like ions can be created by transitions from doubly-excited states of He- and Li-like ions respectively.The satellites to resonance lines $2p_{1/2}$-$1s_{1/2}$ and $2p_{3/2}$-$1s_{1/2}$ are obtained by $2lnl'[LSJ]$-$1snl''[L'S'J']$ transitions with all possible n and l. The satellites to resonance lines $1s2p$ $[^{1,3}P_1]$-$1s^2$ $^1S_0$ are obtained by $1s2lnl'[LSJ]$-$1s^2nl''[L'S'J']$ transitions with all possible n and l. The double excited $2lnl'[LSJ]$ and $1s2lnl'[LSJ]$ states create the satellites to $np_{1/2}$-$1s_{1/2}$, $np_{3/2}$-$1s_{1/2}$ and $1s2p$ $[^{1,3}P_1]$-$1s^2$ $^1S_0$ lines by the $2lnl'[LSJ]$-$1s2l''[L'S'J']$ and $1s2lnl'[LSJ]$-$1s^22l''[L'S'J']$ transitions in He- and Li-like ions.

The occurrence of autoionizing states in atoms and ions has very significant effect on the character of the radiation spectrum of high-temperature astrophysical and laboratory plasma (Boiko *et al.* [1], Dubau *et al.* [2], Bitter *et al.* [3]). Their radiative decay is accompanied by the formation of satellite of the resonance lines in ions of the next ionization degree, which as a rule occupy a narrow spectrum interval and involve information on the plasma state which used for its diagnostics. The theoretical study of autoionizing states of He- and li-like ions is also important for understanding of charge exchange processes as observed in collision experiments between neutral atoms and ions [4, 5, 6, 7, 8, 9]. The

U.I. Safronova.
Department of Physics, University of Notre Dame, Notre Dame, IN 46556, USA.
Telephone: (219) 631-4008, **FAX:** (219) 631-5952, **e-mail:** usafrono@nd.edu
A.A. Vasilyev.
Department of Physics, University of Notre Dame, Notre Dame, IN 46556, USA.
R.K. Smith.
Smithsonian Astrophysical Observatory, 60 Garden St., Cambridge, MA 02138, USA.

satellite spectra have been used as a diagnostic tool to measure the temperature and ionization state of a plasma. The dielectronic data for H- and He- like ions are very important to an accurate calculation of the emission from a hot (10^4 - 10^9 K) collisionally ionized plasma.

Two new X-ray telescopes, the Chandra X-ray Observatory and the XMM-Newton have recently been launched. At 1 keV, Chandra has a maximum resolution of $\lambda/d\lambda$= 1000 [10], while XMM has a maximum resolution of 400 [11]. As we will show, this resolution is sufficient to resolve some of the dielectronic lines. These lines are temperature/ionization diagnostics because the intensity of the satellite lines is proportional to the ion population of the parent ion (and is strongly dependent upon the electron temperature), while the resonant line intensity is proportional to the population of the daughter ion. In addition, the small separation between the lines minimizes the effect of calibration uncertainties on the measured line ratio. With theoretical models such as those discussed here, these line ratios will be excellent diagnostics of the plasma conditions.

Few computer programs were created for identification of the high-resolution spectra. The MZ program gives energies, transition probabilities, autoionization rates, and branching ratios with using a many-body perturbation theory. Relativistic, correlation, QED effects were taken into account. A Breit Hamiltonian was used for the calculation of relativistic effects. Correlation effects were obtained by calculation of the second order Feynman diagrams. QED effects were included in the first order approximation. In particular, the MZ program is convenient in providing data for an isoelectronic sequence because a nuclear charge (Z) is included in the program analytically in a form of 1/Z expansion [4].

This paper reports new results for autoionization states of He- and Li-like ions associated with two types of transitions: $2lnl'$-$1snl''$ and $2lnl'$-$1s2l$ (n=4-5, l=0-3) for He-like ions and $1s2lnl'$ - $1s^2nl''$ and $1s2lnl'$-$1s^22l$ (n=4-5, l=0-3) for Li-like ions with Z=5-54.

2. Dielectronic satellite lines

The satellite lines considered here are usually called dielectronic satellites (DS) . Dielectronic recombination (DR) is defined by the following sequence of processes [12]

$$\begin{array}{rcl} X_{Z_S+1}(\alpha_0)+e & \Rightarrow & X_{Z_S}(\gamma) \Rightarrow X_{Z_S}(\gamma') + h\omega(\gamma-\gamma') \\ & \Downarrow & \\ & & X_{Z_S+1}(\alpha') + e' \end{array} \quad (1)$$

where Z_S is the spectroscopic symbol of the ion $X_{Z_S}(\gamma)$, which forms a satellite spectra of the type $\gamma - \gamma'$ with $\omega(\gamma-\gamma')$ frequency. The first step of this process ($X_{Z_S+1}(\alpha_0)+e \Rightarrow X_{Z_S}(\gamma)$) is a free-electron capture into a double excited autoionizing state γ, and the second step is a radiative ($X_{Z_S}(\gamma) \Rightarrow X_{Z_S}(\gamma') + h\omega(\gamma-\gamma')$) and nonradiative ($X_{Z_S}(\gamma) \Rightarrow X_{Z_S+1}(\alpha') + e'$) stabilization. In our specific cases H- and He-like ions, we can rewrite this process in the following ways:

$$\begin{array}{rcl} H(1s)+e & \Rightarrow & He(nln'l') \Rightarrow He(1sn''l'') + h\omega(nln'l' - 1sn''l'') \\ & \Downarrow & \\ & & H(1s) + e' \end{array} \quad (2)$$

$$\begin{array}{rcl} He(1s^2)+e & \Rightarrow & Li(1snln'l') \Rightarrow Li(1s^2n''l'') + h\omega(1snln'l' - 1s^2n''l'') \\ & \Downarrow & \\ & & He(1s^2) + e' \end{array} \quad (3)$$

It should be noted that DR process is not only one to form the $nln'l'$ and $1snln'l'$ autoionizing states. There is another process competing with DR, namely the excitation with an electron impact process [12]

$$X_{Z_S}(\gamma_0) + e \Rightarrow X_{Z_S}(\gamma) + e' \Rightarrow X_{Z_S}(\gamma') + e'' + h\omega(\gamma - \gamma'). \tag{4}$$

where $\gamma_0 = 1s^2 2l$, $\gamma = 1s2l'nl'$, and $\gamma' = 1s^2 nl$ for Li-like ions. Below we consider satellite lines obtained by the DR process. The relative intensity Q_d of the dielectronic satellite lines of the type $\gamma - \gamma'$ is

$$Q_d(\gamma\gamma') = g_\gamma A_a(\gamma) K(\gamma\gamma'), \qquad K(\gamma\gamma') = \frac{A_r(\gamma\gamma')}{A_r(\gamma) + A_a(\gamma)}, \qquad A_r(\gamma) = \sum_{\gamma''} A_r(\gamma\gamma''), \tag{5}$$

where $A_r(\gamma\gamma')$ is radiative transition probabilities, $A_a(\gamma)$ is autoionizing rates of γ states, and g_γ is a statistical weight of these states. Here γ=$2lnl'$, γ'=$1snp$, $1s2p$ for He-like ions and γ=$1s2lnl'$, γ'=$1s^2np$, $1s^22p$ for Li-like ions. Some details of the calculation of the relative intensity factor, radiative and autoionizing rates, and wavelengths of dielectronic satellite lines of He- and Li-likes ions are given below.

3. Method

This work is a part of continuing effort to carry out accurate calculations of different atomic characteristics for two-electron and three-electron systems using the MZ code [4], [5]. The MZ application is based on the perturbation theory method developed on a Coulomb basis. The energy matrix in this method (called 1/Z method or Z-expansion) is represented as an expansion on Z, where Z is the nuclear charge. Because of the use of a Coulomb basis the expansion coefficients are the same for all terms of isoelectronic sequence. This is an important advantage of this method. The interaction of terms and configurations inside one complex is taken into account already in the first order coefficients; a complex means a group of configurations with the same parity and the same principal quantum numbers. The interaction of the configurations from different complexes is considered in the next orders of perturbation theory. The relativistic corrections are calculated in the framework of Breit operator. In addition the radiative and high-order relativistic corrections are also taken into account. In the MZ theory the energy matrix can be represented in the form [13]:

$$\begin{aligned} E(aLSJ, a'L'S'J) \quad = \quad & \delta(LS, L'S') \left[\delta(a,a')E_0^N Z^2 + E_1^N Z + E_2^N Z + E_3^N/Z + \right. \\ & \left. \frac{\alpha^2}{4}(Z-\sigma^R)^3\left(\delta(a,a')E_0^R Z + E_1^R\right)\right] + \\ & \frac{\alpha^2}{4}(Z-\sigma^S)^3\left[E_{SO}^{(0)} Z B_1 + E_{SO}^{(1)} B_1 + E_{SA}^{(0)} B_1 + E_{SS}^{(0)} B_2\right]. \end{aligned} \tag{6}$$

Here a,a' designate both configurations, LSJ are the orbital, spin and total angular momentum of the system, Z is a nuclear charge, α is a fine structure constant (1/137.0539 in a u.).

The calculation of every coefficient in $E(aLSJ, a'L'S'J)$ is carried out by means of the Feynman diagram technique [13]. The coefficients E_i^N determine the non-relativistic part of energy, the three next coefficients: σ^R, E_0^R and E_1^R give the relativistic shift of the term, defined by the Breit Hamiltonian and including the dependence of mass on velocity, contact term and orbit-orbit interaction. Finally, the coefficients σ^S, $E_{SO}^{(i)}$, $E_{SO}^{(1)}$, $E_{SA}^{(0)}$ and $E_{SS}^{(0)}$ determine the fine structure splitting of terms and consists of three operators: spin-orbit , spin-other-orbit and spin-spin interactions. We calculated these coefficients for the $2l2l'$, $2l3l'$, $1s2l2l'$, and $1s2l3l'$ states. The values of these coefficients for $2lnl'$,

$1s2lnl'$ with $n > 3$ are obtained by screening representation (see Appendix). After diagonalization of the energy matrix, we obtain the coefficients $C^J(aLS, a'L'S')$ for the intermediate coupling scheme and the energy eigenvalues $E^J(aLS)$.

In an intermediate-coupling scheme, the autoionizing rate of a level $aLSJ$ is equal to: [4], [5]

$$A_a(aLSJ) = \sum_{L'S'} \sum_{a'a''} C^J(aLS, a'L'S')\Gamma^N(a'L'S', a''L'S')C^J(a''L'S', aLS), \tag{7}$$

$$\Gamma^N(aLS, a'LS) = 2\pi \sum_{a_0 k\ell} \gamma(aLS, a_0 k\ell LS)\gamma(a'LS, a_0 k\ell LS), \tag{8}$$

where

$$\gamma(aLS, a_0 klLS) = \sqrt{\frac{1}{k}}\, \langle aLS| \sum_{i>j} \frac{1}{r_{ij}} |a_0 klLS\rangle\,. \tag{9}$$

Here k defines a moment of ejected electron for the continuous state $a_0 klLS$. Let us remind that for $2l'nl$ states a_0=$1s$ only.

The radiative transition probabilities between $aLSJ$ and $a'L'S'J'$ levels is equal to: [13]

$$\begin{aligned} A_r(aLSJ, a'L'S'J') \quad = \quad & \frac{2}{(2J+1)} \left[E^J(als) - E^{J'}(a'L'S')\right]^3 \\ & \times \left[\sum_{a_1 L_1 S_1} \sum_{a'_1 L'_1} B(L_1S_1J, L'_1S'_1J)C^J(aLS, a_1L_1S_1)C^{J'}(a'_1L'_1S'_1, a'L'S') \right. \\ & \left. \times\, \frac{1}{Z}\varepsilon(L_1S_1J, L'_1S'_1J) \left\{1 + \frac{1}{Z}\tau(L_1S_1J, L'_1S'_1J)\right\} \right]^2 . \end{aligned} \tag{10}$$

Here $\tau(L_1S_1J, L'_1S'_1J)$ is the first order correction in electron interaction for the dipole matrix element and $B(L_1S_1J, L'_1S'_1J)$ is an angular factor [13].

4. Result and discussion

We calculate wavelengths, radiative transition probabilities $A_r(aLSJ, a'L'S'J')$, autoionizing rates $A_a(aLSJ)$ and relative intensity factors $Q_d(aLSJ, a'L'S'J')$ in He- and Li-like ions associated with two types of transitions: $2lnl'$ - $1snl''$ and $2lnl'$- $1s2l$ (n=4-5, l=0-3) for He-like ions and $1s2lnl'$ - $1s^2nl''$ and $1s2lnl'$- $1s^22l$ (n=4-5, l=0-3) for Li-like ions with Z=5-54. Our results are presented as function of Z for $A_r(aLSJ, a'L'S'J')$, $A_a(aLSJ)$, and $Q_d(aLSJ, a'L'S'J')$ for a limited number of transitions. Complete results with including all transitions are shown for satellites with Z=7 and 8.

4.1. Z-dependences of the atomic characteristics for 2l5l' and 1s2l5l' states of two- and three-electron systems

The investigation of Z-dependences is the subject of great importance for the atomic physics because of the possibility to study the changing of the contributions of correlation, relativistic and radiative effects to the atomic characteristics with Z. As was already mentioned above only parity and total angular momentum J of atomic system determine state; all possible configurations, LS, together with intermediate $L_{12}S_{12}$ can be included in a *complex*. For example, the even parity $1s2sns$, $1s2pnp$, $1s2snd$ configurations can not mix with the odd parity $1s2snp$, $1s2pns$, $1s2pnd$ configurations. The even parity *complex* with J=5/2 consists of 14 states, i.e.

$$1s2p(^3P)5p[^4P],\quad 1s2p(^1P)5p[^2D],\quad 1s2p(^3P)5p[^2D],\quad 1s2p(^3P)5p[^4D], \tag{11}$$
$$1s2s(^1S)5d[^2D],\quad 1s2s(^3S)5d[^2D],\quad 1s2s(^3S)5d[^4D],\quad 1s2p(^1P)5f[^2D],\quad 1s2p(^3P)5f[^2D],$$
$$1s2p(^3P)5f[^4D],\quad 1s2p(^1P)5f[^2F],\quad 1s2p(^3P)5f[^2F],\quad 1s2p(^3P)5f[^4F],\quad 1s2p(^3P)5f[^4G].$$

For the following discussion it is more convenient to use letters for the designations of states in a *complex* [4], [14, 15]. We use the following notations, i.e.

$$\begin{aligned} G' &= 1s2s(^1P)5d,\quad N' = 1s2s(^3P)5d,\quad F' = 1s2p(^3P)5p,\quad M' = 1s2p(^3P)5p, \\ V' &= 1s2p(^3P)5f,\quad W' = 1s2p(^3P)5f,\quad P = 1s^22p,\quad P' = 1s^25p,\qquad P' = 1s^25p. \end{aligned} \tag{12}$$

Together with these notations for configurations and intermediate momentum describing two-electron states, we use the designation $(2S+1)(2l+1)(2J+1)$ instead of $^{2S+1}L_J$. Thus, we can rewrite the states of the even complex with J=5/2:

$$\begin{aligned} &M'436,\quad F'256,\quad M'256,\quad M'456,\quad G'256,\quad N'256,\quad N'456, \\ &V'456,\quad W'256,\quad W'456,\quad V'276,\quad W'276,\quad W'476,\quad W'496. \end{aligned} \tag{13}$$

This classification is used in Figs. 1, 2, and 3. It is necessary to note that we keep designations of levels using the largest mixing coefficient from $C^J(aLS, a'L'S')$ which were obtained as a result of diagonalization of an energy matrix inside a *complex*. This procedure works well for small Z values in the range of Z=5 to 15 but this method is rather difficult for Z= 20- 40. For higher Z values it is more convenient to use jj-coupling scheme together with the designations that have been used in Ref. [16]. The intermediate values of Z (Z=20-40) are the most complicated ones for a clear-cut identification of spectra because the contributions resulting from correlation and relativistic effects are almost equal. For small Z the correlation effects play a more important role than relativistic ones. On the other hand for high Z values the relativistic effects dominate over correlation contributions. Figs. 1 and 2 display the obtained relative intensity factors, $Q_d(1s2l(L_{12}S_{12})5l'[^{2,4}L_{5/2}]-1s^25p[^2P_{3/2}])$ and $Q_d(1s2l(L_{12}S_{12})5l'[^{2,4}L_{5/2}]-1s^22p[^2P_{3/2}])$ for different kinds of indexes $L_{12}S_{12}, l, l'$ and L. Due to space limitations we can show Z-dependences for a limited number of $Q_d(1s2l(L_{12}S_{12})5l'[^{2,4}L_J] - 1s^25l''[^2l''_{J'}])$ and $Q_d(1s2l(L_{12}S_{12})5l'[^{2,4}L_J] - 1s^22l''[^2l''_{J'}])$ with different $L_{12}S_{12}$, l, l', l'', J, J' and L indexes. It should be noted, that the number of the $1s2l(L_{12}S_{12})n'l'[^{2,4}L_J] - 1s^2n''l''[^2l''_{J'}])$ transitions increases very rapidly with increasing principal quantum number n' and n''. There are only the 22 transitions with $n' = n''$=2, but 202 transitions with n' =3, n''=2 and 3, and 289 transitions with n' =4, n''=2 and 4, and so on.

We can see rather complicated Z-dependencies with maximums and minimums for $Q_d(\gamma\gamma')$, relative intensity factors Figs. 1 and 2 and for $A_r(\gamma\gamma')$, radiative transition probabilities Fig. 3. Some maximums and minimums are the same for $Q_d(\gamma\gamma')$ and $A_r(\gamma\gamma')$. Some new maximums and minimums for $Q_d(\gamma\gamma')$ should be explained by maximums and minimums for $A_a(\gamma)$. These maximums and minimums for all curves $A_a(\gamma)$, $A_r(\gamma\gamma')$ and $Q_d(\gamma\gamma')$ are observed for intermediate values of Z (Z=15 -25), where correlation and relativistic effects give comparable contribution. Some crossing of levels is shown in Fig. 3. The level $M'436$ is crossed with the level $M'456$ in the range of Z=39-40, then with the level $W'276$ in the range of Z=45-46 and Z=51-52. This crossing could be omitted by changing the label of levels [17].

The results for He-like ions are shown in Figs. 4-8. We used $(2S+1)(2l+1)(2J+1)$ instead of $^{2S+1}L_J$ and the following designation for configurations:

$$\begin{aligned} E' &= 2s5s,\quad F' = 2p5p,\quad G' = 2s5d,\quad J' = 2p5f, \\ P &= 1s2p,\quad P' = 1s5p,\quad H' = 1s5f. \end{aligned} \tag{14}$$

For example, $F'335 - P'133$ transition shown in Fig. 4 denotes $2p5p^3P_2 - 1s5p^1P_1$ transition. All levels are divided for parity and quantum number of system J, that means levels included in one *complex*. Below, we consider even parity *complex* with J=2 that includes the following 8 levels: $F'335,\ F'155,\ F'355,\ G'155,\ G'355,\ J'155,\ J'355,\ J'375$. There are 9 channels for radiative transitions from these levels: $P133,\ P333,\ P335,\ P'133,\ P'333,\ P'335,\ H'375, H'177$, and $H'377$. For illustration of our result, we show transitions in two channels only: $P'133$ (Figs. 4 and 7) and $H'377$ (Figs. 5 and 8). As can seen from Figs. 4 and 5 , Z-dependences of the relative intensity factors, $Q_d(\gamma\gamma')$ are not smooth. There are the crossing levels and singularities with deep minima. That corresponds to singularities in the radiative transition probabilities (Figs. 7 and 8) and the autoionizing rates Fig. 6. Of course, all singularities are provided by complicated mixing of states in the *complex* (including configuration mixing and intermediate coupling).

We emphasize that $Q_d(\gamma\gamma')$ is a very crucial parameter for dielectronic satellite lines and determines the relative intensity of each satellite lines in spectra produced by various laboratory and solar plasma. These intensities are rapidly changing with Z for different types of transitions (see Figs. 4 and 5). Consequently, the form of satellite spectra is strongly affected by Z and theoretical calculations are necessary to predict which lines are prominent and which lines can disappear at specific Z values. These data will be interesting to check by experiment, if it is possible, by observing the whole isoelectronic sequence including the lower and higher Z.

4.2. Dielectronic satellites in N^{5+}, O^{6+}, N^{4+}, and O^{5+}

Dielectronic satellites are shown in Figs. 9-18. In Figs. 9-11, 12-14, 15-16, and 17-18, we show synthetic spectra for N^{5+}, O^{6+}, N^{4+}, and O^{5+} accordingly. Dielectronic satellites $2l2l'-1s2l''$, $2lnl'-1snl$" with n=2-5, and $2lnl' - 1s2l$" with n=3-5 for N^{5+} and O^{6+} are compared in Figs. 9 and 13, Figs. 10 and 14, Figs. 11 and 12 accordingly. Dielectronic satellites $1s2lnl' - 1s^2nl$" with n=2-5, and $1s2lnl' - 1s^22l$" with n=3-5 for N^{4+} and O^{5+} are compared in Figs. 15 and 17, Figs. 16 and 18 accordingly. To construct these spectra, we use Gaussian line profile.

$$Q_d(\lambda) = Q_d(\lambda_0)2\sqrt{\frac{\ln 2}{\pi}}\frac{\lambda_0^2}{\lambda^2\delta\lambda_0}\exp\left[-4\ln 2\frac{(\lambda_0^2-\lambda\lambda_0)^2}{(\lambda\delta\lambda_0)^2}\right], \tag{15}$$

where $\delta\lambda_0$ is equal to 0.02 in our synthetic spectra.

In Figs. 9, 13, we present satellite spectra with including only n=2 states ($2l2l' - 1s2l''$). These satellite spectra are composed of the 5-7 lines in the interval of 0.5-1.1Å. In Figs. 10, 14, 15, and 17, we demonstrate the effect of high n contribution. As can seen from these spectra, some of the lines are not completely resolved in the small 0.2Åinterval. The wavelengths of these lines are almost equal to the wavelengths of resonance lines ($2p - 1s$ for N^{5+} and O^{6+} spectra or $1s2p - 1s^2$ for N^{4+} and O^{5+} spectra). That leads to the broadening of resonance lines. In Figs. 11, 12, 16, and 18, we illustrate contribution of $2lnl'-1s2l''$, and $1s2lnl'-1s^22l''$ transitions. As can seen from these synthetic spectra, they contain from three group of lines obtained from $2lnl' - 1s2l''$, and $1s2lnl' - 1s^22l''$ transitions with n=3, 4, and 5.

5. Conclusion

In summary, a systematic study of the relative intensities of dielectronic satellite lines determined by radiative transition probabilities and autoionization rates is performed. All possible $2lnl'$ - $1snl'$, $2lnl'$ - $1s2l$ (n=4-5, l=0-3) transitions in He-like ions and $1s2lnl'$ - $1s^2nl'$, $1s2lnl'$ - $1s^22l$ (n=4-5, l=0-3) transitions in Li-like ions are included.

The radiative transition probabilities, autoionization rates and relative intensity factors are shown in graphical form as Z-dependences for a broad range of Z (Z-5-54). It was observed that these characteristics change very sharply with Z due to redistribution between contribution of relativistic and correlation effects.

The synthetic spectra for dielectronic satellites in N^{5+}, O^{6+}, N^{4+}, and O^{5+} are presented. In these figures, we demonstrate the effect of the high n contribution. Some of these lines are not completely resolved in the small 0.2Åinterval. The wavelengths of these lines are almost equal to the wavelengths of resonance lines ($2p - 1s$ for N^{5+} and O^{6+} spectra or $1s2p - 1s^2$ for N^{4+} and O^{5+} spectra). That leads to the broadening of resonance lines.

Acknowledgments

The work of UIS was supported in part by support by Grant No. 44514 from Smithsonian Astrophysical Observatory . RKS acknowledges support from NASA Contract NAS8-39073 and NASA Grant NAG5-3559.

Appendix. Screening representation in 1/Z-expansion method

The MZ code is based on perturbation theory method with coulomb basis. In this method (1/Z method or 1/Z-expansion method) an energy matrix is represented in the form of 1/Z-expansion series (Z is a nuclear charge) and the calculation of every coefficient of this series is carried out by means of the Feynman diagram technique [5]. As an advantage of this method the coefficients are constant for whole isoelectronic sequence and they depend only on electronic state. We can note that mixing of configurations inside of one complex is taken into account by the first order coefficients of considered series. The complex of states means a group of configurations with the same parity and set of principal quantum numbers (2s3p + 2p3s + 2p3d, for example). The mixing between configurations of different complexes is considered by the second and other higher order diagrams of perturbation theory method. Breit operators are responsible for relativistic contribution. Radiative corrections (Lamb shift) and other high order over (where is the fine structure constant and 1/α=137.0359) are also take into account by MZ code. We will not discuss calculation of all 1/Z coefficients in detail (see an example in papers [4], [6], [9, 14, 15] and monograph [5]). Purpose of this appendix is to discuss the screening representation in MZ code.

It is convenient to represent the energy matrix in a form:

$$E(aLSJ, a'L'S'J) = \delta(LS, L'S')\left[E^N(aLS, a'LS) + E^R(aLS, a'LS)\right] + E^S(aLSJ, a'L'S'J), \quad (16)$$

where a, a' describe configurations, LSJ are momentum of considered system. The three components in Eq.(16) are represented nonrelativistic (E^N(aLS,a'LS)) part of energy, relativistic part (E^R(aLS,a'LS)) concerning shift of energy and relativistic splitting (E^S (aLS,a'LS)). Each of these components can be divide on two parts for core contribution and contribution described by interaction of optical electron nℓ with core. General formulas for E^N(aLS,a'LS), E^R(aLS,a'LS) and E^S(aLS,a'LS) were given in paper by Safronova et al[9]. Here we represent formulas for two-electron system, as 1snℓ and 2ℓ'nℓ.

i) Diagonal matrix elements:

$$E^N(p\ell' n\ell LS, p\ell' n\ell LS) = -\frac{Z^2}{2p^2} - \frac{[Z - \sigma(n\ell LS)]^2}{2n^2} + E_2'(p\ell' n\ell LS), \qquad p = 1, 2 \quad (17)$$

$$E^R(p\ell' n\ell LS, p\ell' n\ell LS) = \frac{\alpha^2}{4} Z^4 E_0^R(p\ell') + \frac{\alpha^2}{4} Z E_0^R(n\ell)\left[Z - \sigma^R(n\ell LS)\right]^3, p = 1, 2 \quad (18)$$

$$E^S(p\ell_1 n\ell_2 LSJ, p\ell_1 n\ell_2 L'S'J) = \frac{\alpha^2}{4} Z^4 E_0^S(p\ell_1) + \frac{\alpha^2}{4}\left[Z - \sigma^S(LS, L'S')\right]^3$$

$$\times\left[Z E_0^S(n\ell_2) + \varepsilon_{SO} Q_1 + \varepsilon_{SS} Q_2\right], p = 1, 2. \quad (19)$$

ii) Non-diagonal matrix elements:

$$E^N(p\ell_1 n\ell_2 LS, p\ell_3 n\ell_4 LS) = ZE_1'(p\ell_1 n\ell_2 LS, p\ell_3 n\ell_4 LS) + E_2'(p\ell_1 n\ell_2 LS, p\ell_3 n\ell_4 LS), \tag{20}$$

$$E^R(p\ell_1 n\ell_2 LS, p\ell_3 n\ell_4 LS) = \frac{\alpha^2}{4} Z^3 R_1'(p\ell_1 n\ell_2 LS, p\ell_3 n\ell_4 LS), \tag{21}$$

$$E^S(p\ell_1 n\ell_2 LSJ, p\ell_3 n\ell_4 L'S'J) = \frac{\alpha^2}{4}\left[Z - \sigma^R\right]^3 \left[\varepsilon_{SO} Q_1 + \varepsilon_{SS} Q_2\right]. \tag{22}$$

Screening constants (σ, σ^R, σ^S) are determined by ratio of the first and zero order corrections:

$$\sigma(n\ell LS) = -\frac{E_1(p\ell' n\ell LS)}{2E_0(n)} = n^2 E_1((p\ell' n\ell LS), \tag{23}$$

$$\sigma^R(n\ell LS) = \sigma(n\ell LS) + \frac{R_1'(p\ell' n\ell LS)}{3E_0^R(n\ell)}, \tag{24}$$

$$\sigma^S(LS, L'S') = -\frac{\varepsilon_1(p\ell_1 n\ell_2; LSL'S')}{3\varepsilon(n\ell_2)}. \tag{25}$$

Zero order coefficients are equal to

$$E_0(n) = -\frac{1}{2n^2}, \tag{26}$$

$$E_0^R(n\ell) = -\frac{2}{n^3}\left[\frac{2}{2\ell+1} - \frac{3}{4n} - \delta(\ell,0)\right], \quad E_0^R(1s) = -\frac{1}{2}, E_0^R(2s) = -\frac{5}{32}, E_0^R(2p) = -\frac{7}{96}, \tag{27}$$

$$E_0^S(n\ell_2) = \varepsilon(n\ell_2) q_1(L\ell_2\ell_1), \quad \varepsilon(n\ell) = \frac{2}{n^3}\sqrt{\frac{6}{\ell(\ell+1)(2\ell+1)}}, \tag{28}$$

where the angular part is described by 6j-Wigner coefficients:

$$q_1(L\ell_1\ell_2) = Q_1(L\ell_1\ell_2) Q_1(S\frac{1}{2}\frac{1}{2})\sqrt{(2L+1)(2L'+1)(2S+1)(2S'+1)}, \tag{29}$$

$$Q_r = Q_r(LSJ) = (-1)^{L'+S+1}\left\{\begin{array}{ccc} L & S & J \\ S' & L' & r \end{array}\right\}. \tag{30}$$

Coefficients for determination of E^N(aLS,a'LS), E^R(aLS,a'LS) and E^S(aLS,a'LS) for a, a'=1snℓ (n=2, 3, 4) and a, a'=2ℓ'nℓ (n=3, 4) are given Ref. [9].

Let us explain about asymptotic behavior of these coefficients. The first and the second order corrections for non-relativistic part of an energy include 1/n^2 term as a leading term:

$$E_1(p\ell' n\ell) = \frac{1}{n^2} + E_1'(p\ell' n\ell), \tag{31}$$

$$E_2(p\ell' n\ell) = -\frac{1}{n^2} + E_2'(p\ell' n\ell) - E_1'(p\ell' n\ell) - \frac{n^2}{2}\left[E_1'(p\ell' n\ell)\right]^2. \tag{32}$$

As a result the leading term for $E_1'(p\ell' n\ell)$ and $E_2'(p\ell' n\ell)$ expressions is proportional 1/n^3 instead 1/n^2 for $E_1(p\ell' n\ell)$ and $E_2(p\ell' n\ell)$. For relativistic shift contribution, the changing $R_1(p\ell' n\ell)$ to $R_1'(p\ell' n\ell)$ leads only to decreasing of this contribution ($R_1'(p\ell' n\ell) \simeq R_1(p\ell' n\ell)$/10). As a result, the representation of the energy in the form of Eqs.(16-19) removes all terms proportional to $1/n^2$, and the additional coefficients in Eqs.(16-19) are proportional $1/n^3$. It is possible in this case to obtain coefficients in Eqs.(16-19) for large n by using asymptotic formula and data for these coefficients calculated for previous $n=n_0$: $E'_k(n) = E'_k(n_0)\left(\frac{n_0}{n}\right)^3$, $R'_1(n) = R'_1(n_0)\left(\frac{n_0}{n}\right)^3$, $\varepsilon_{SO}(n) = \varepsilon_{SO}(n_0)\left(\frac{n_0}{n}\right)^3$, $\varepsilon_{SS}(n) = \varepsilon_{SS}(n_0)\left(\frac{n_0}{n}\right)^3$.

In this paper we used data calculated for s, p, d states with n_0=3 (1sns, 1snp, 1snd, 2ℓns, 2ℓnp, 2ℓnd) and for f states with n_0=4 (1snf, 2ℓnf). As a result we obtain values of for s, p, d, f states as function of n, that allow us to create energy matrix for these states with arbitrary n.

References

1. V.A. Boiko, A.Ya. Faenov, S.A. Pikuz and U.I. Safronova. Mon. Not. R. astr. Soc. **181**, 107 (1977).
2. J. Dubau, M. Loulergue and L. Steenman-Clark. Mon. Not. R. astr. Soc. **190**, 125 (1980).
3. M. Bitter, *et al.*. Phys. Rev. A **29**, 661 (1984).
4. L.A. Vainshtein and U.I. Safronova. Atomic Data and Nuclear Data Tables **21**, 49 (1978), **25**, 311 (1980).
5. E.V. Aglitskii and U.I. Safronova. Spectroscopy of autoionizing states of multicharged ions. Energoatomizdat, Moscow. 1985.
6. U.I. Safronova. Physica Scripta T **26**, 59 (1989).
7. M. Cornille, J. Dubau, F. Bely-Dubau, P. Faucher, I.A. Ivanov, U.I. Safronova and J. Nilsen. J. Phys. B **23**, 4451 (1990).
8. J. Nilsen, M. Cornille, J. Dubau, F. Bely-Dubau, P. Faucher, I.A. Ivanov, and U.I. Safronova. J. Quant. Spectrosc. Radiat. Transfer **48**, 61 (1992).
9. U.I. Safronova and W.R. Johnson. Physica Scripta **58**, 116 (1998).
10. The Chandra Proposers' Observatory Guide, V2.0, prepared by Chandra X-ray Center (March 15, 2000), p 174. On the web at http://asc.harvard.edu/udocs/docs/POG/MPOG/index.html (The actual resolving power plot is at http://asc.harvard.edu/udocs/docs/POG/MPOG/node13.html#fg:hetg-res)
11. The XMM Users' Handbook, V1.1, edited by M. Dahlem (January 18, 1999), p.56 On the web at http://astro.estec.esa.nl/XMM/user/uhb/xmm_uhb.html (The actual resolving power plot is at http://astro.estec.esa.nl/XMM/user/uhb/XMM_UHB/node45.html#fig:rgs_specres3)
12. L.A Vainshtein, I.I. Sobelman, and E.A. Yukov. Excitation of Atomic Spectral Line Broadering. Springer-Verlag, Berlin. 1981.
13. U.I. Safronova and V.S. Senashenko. Theory of spectra of multicharged ions. Energoatomizdat, Moscow. 1984.
14. U.I. Safronova, A.S. Shlyaptseva and I.E. Golovkin. Physica Scripta **52**, 277 (1995).
15. U.I. Safronova, A.S. Shlyaptseva and I.E. Golovkin. Physica Scripta **T73**, 50 (1997).
16. M.S Safronova, W.R. Johnson and U.I. Safronova. Phys. Rev. A **53**, 4036 (1996).
17. U.I. Safronova, M.S. Safronova, R. Bruch and L.A. Vainshtein. Physica Scripta **51**,471 (1995).

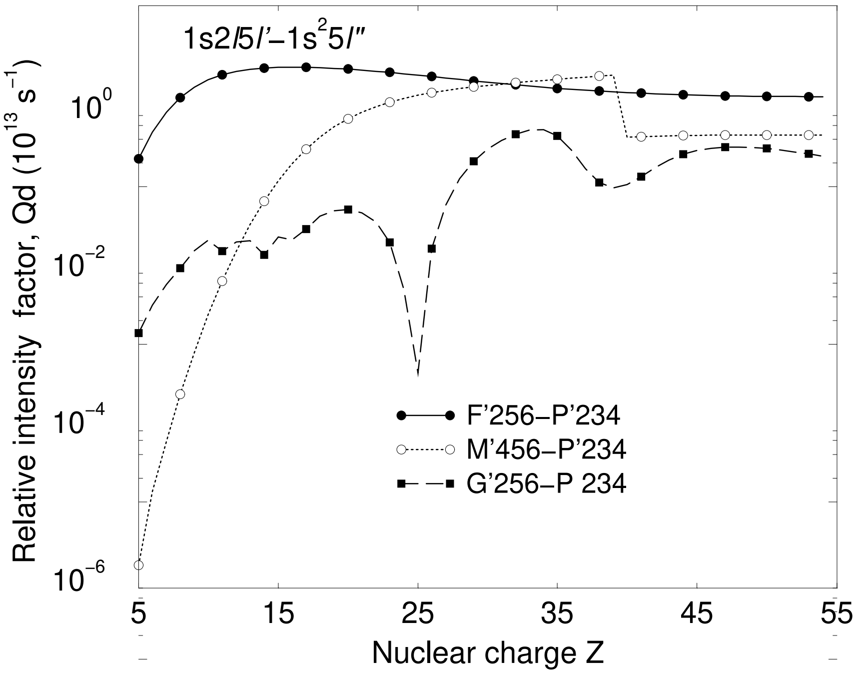

Fig. 1. Relative intensity factor Q_d for $1s2l5l' - 1s^25l''$ transitions in Li-like ions as function of Z

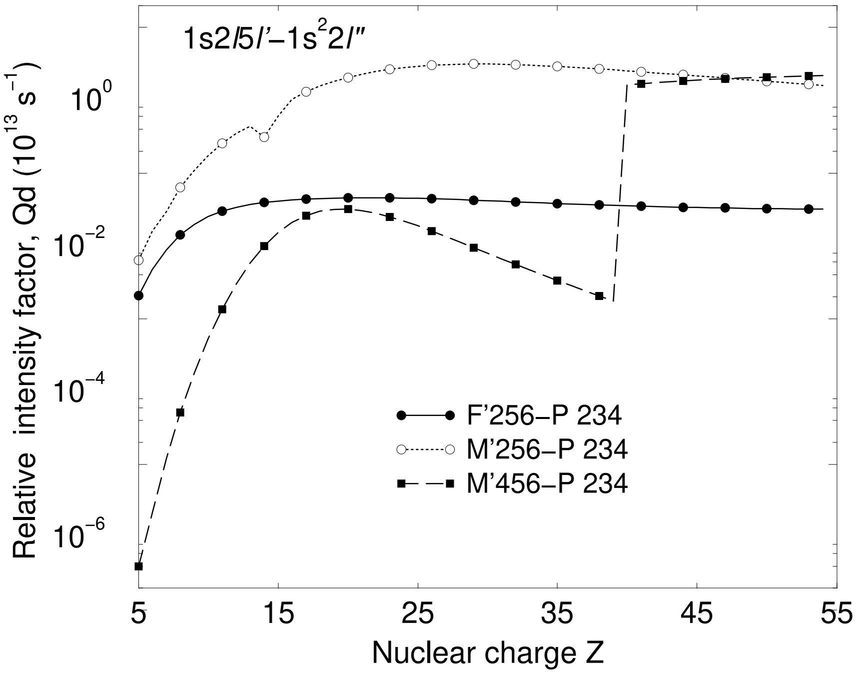

Fig. 2. Relative intensity factor Q_d for $1s2l5l' - 1s^22l''$ transitions in Li-like ions as function of Z

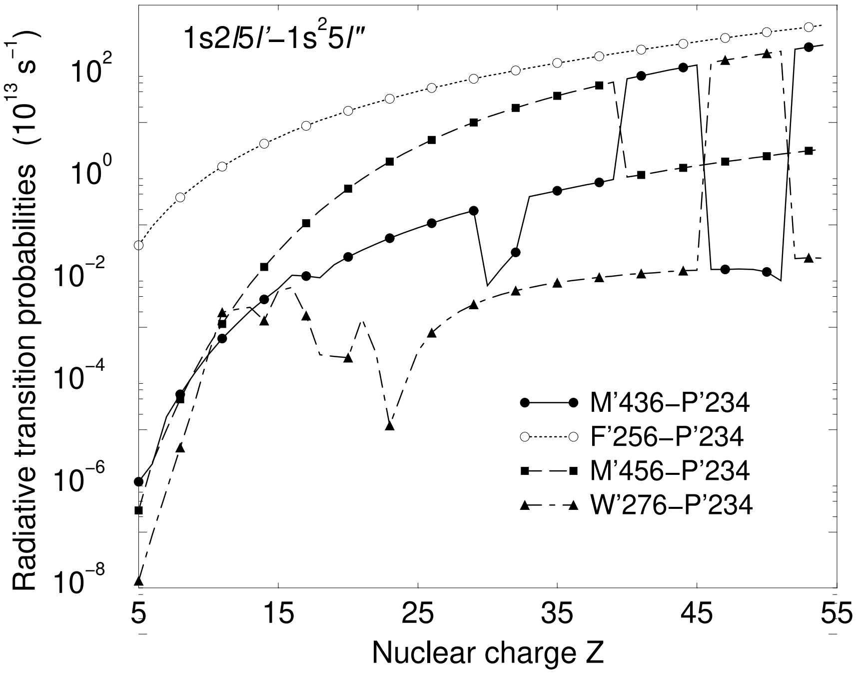

Fig. 3. Transition probabilities $A_r(1s2l5l'\ ^{2,4}L_{5/2} - 1s^25p\ ^2P_{3/2})$ in Li-like ions as function of Z

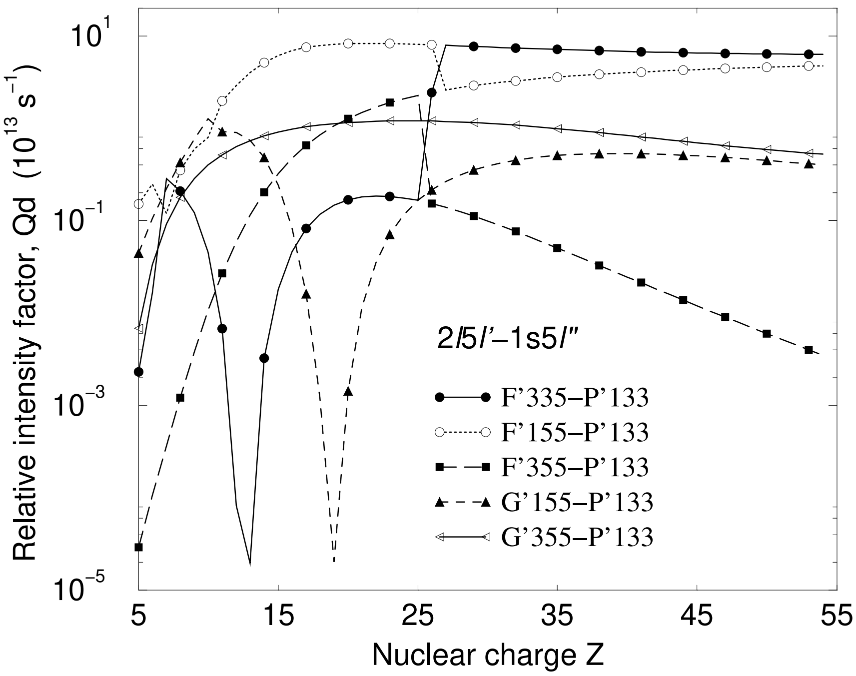

Fig. 4. Relative intensity factor Q_d for $2l5l' - 1s5l''$ transitions in He-like ions as function of Z

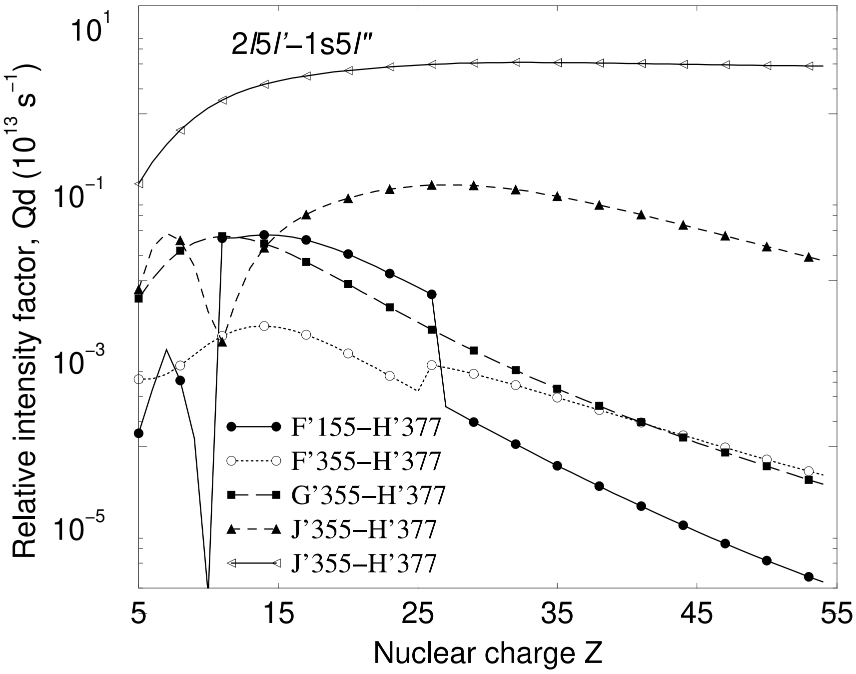

Fig. 5. Relative intensity factor Q_d for $2l5l' - 1s5l''$ transitions in He-like ions as function of Z

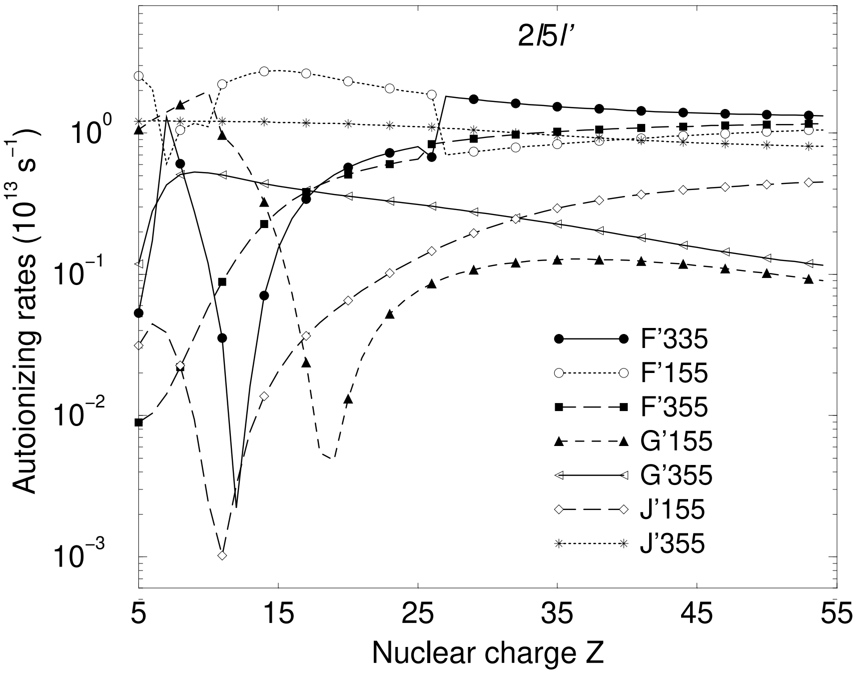

Fig. 6. Autoionizing rates of even parity states with J-2 in He-like ions as function of Z

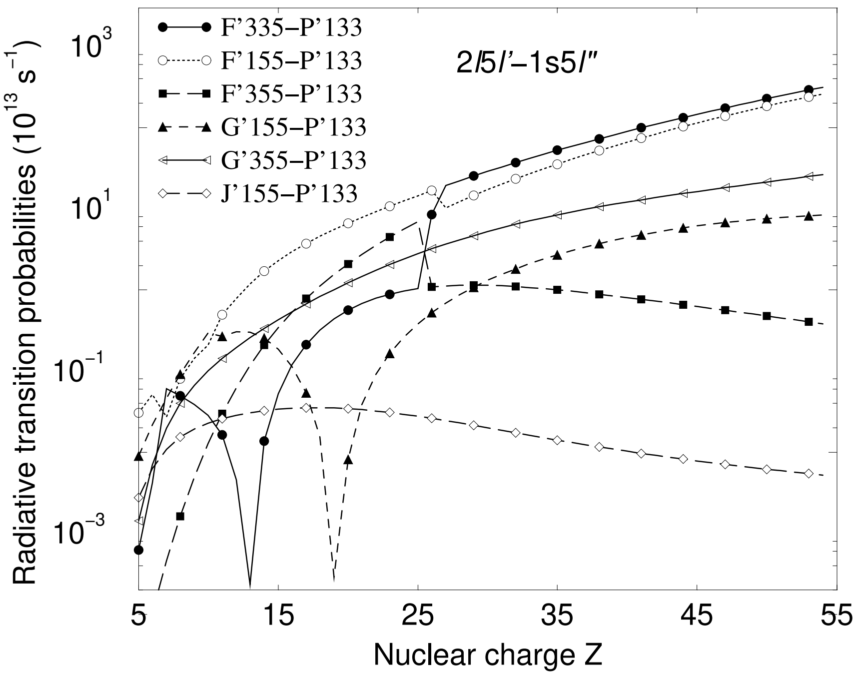

Fig. 7. Transition probabilities $A_r(2l5l'\ ^{1,3}L_2 - 1s5p\ ^1P_1)$ in He-like ions as function of Z

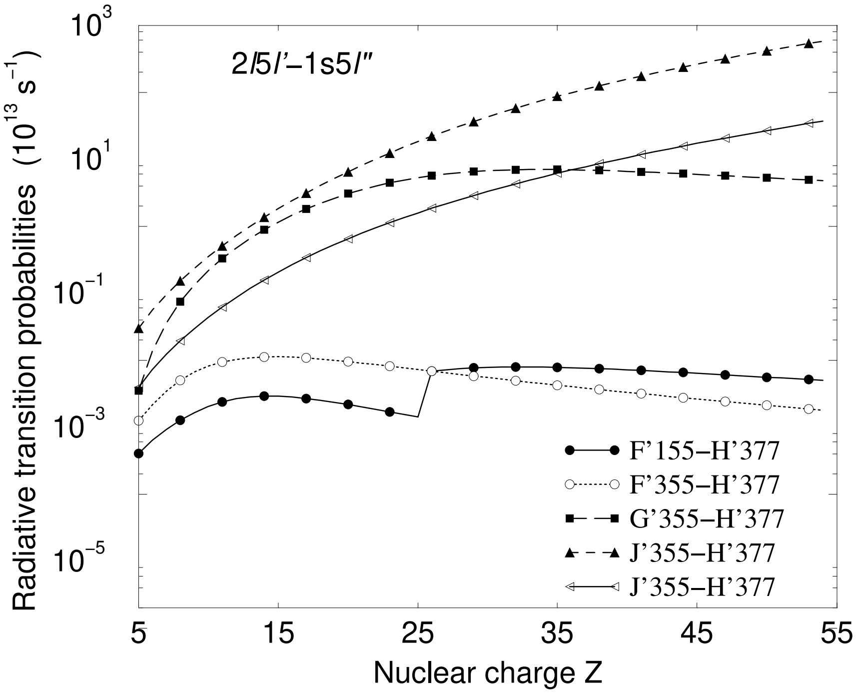

Fig. 8. Transition probabilities $A_r(2l5l'\ ^{1,3}L_2 - 1s5f\ ^3F_2)$ in He-like ions as function of Z

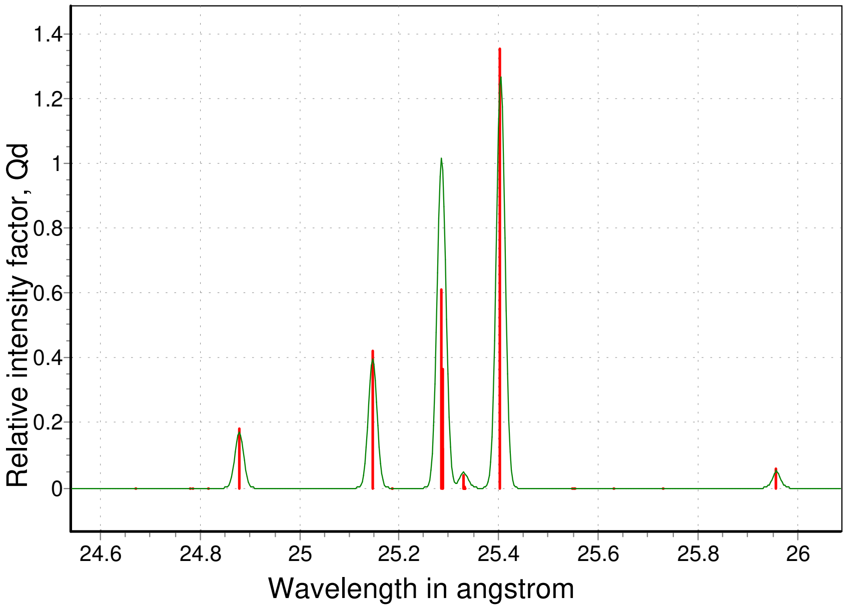

Fig. 9. Dielectronic satellites $2l2l' - 1s2l''$ in N^{5+}

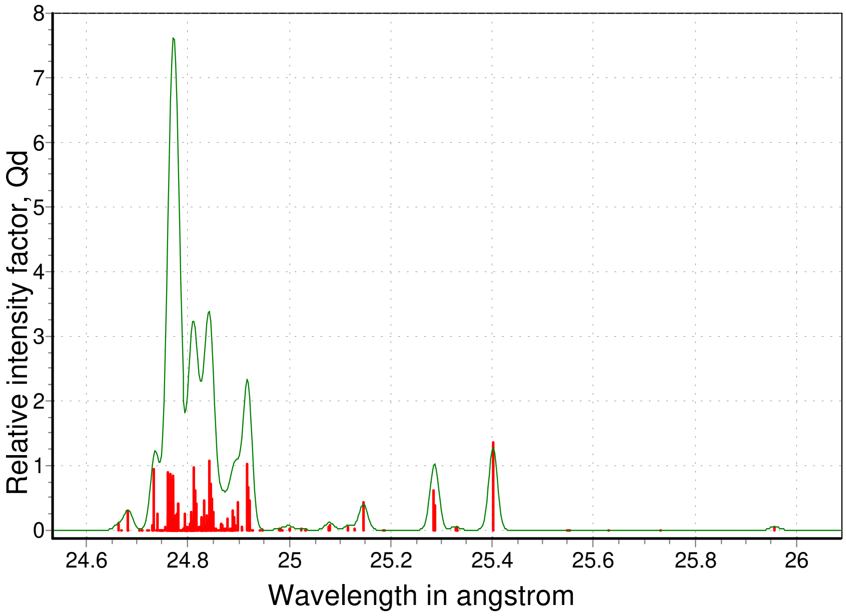

Fig. 10. Dielectronic satellites $2lnl' - 1snl$" with n=2-5 in N^{5+}

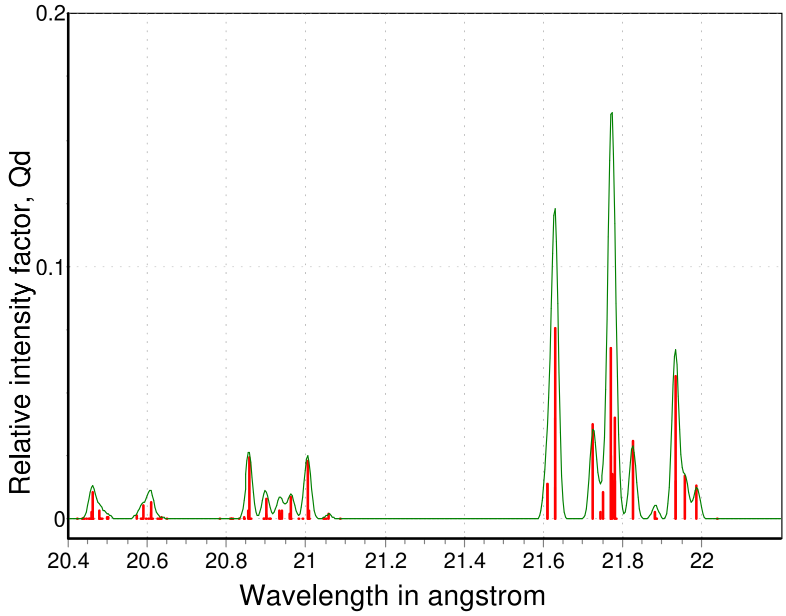

Fig. 11. Dielectronic satellites $2lnl' - 1s2l"$ with n=3-5 in N^{5+}

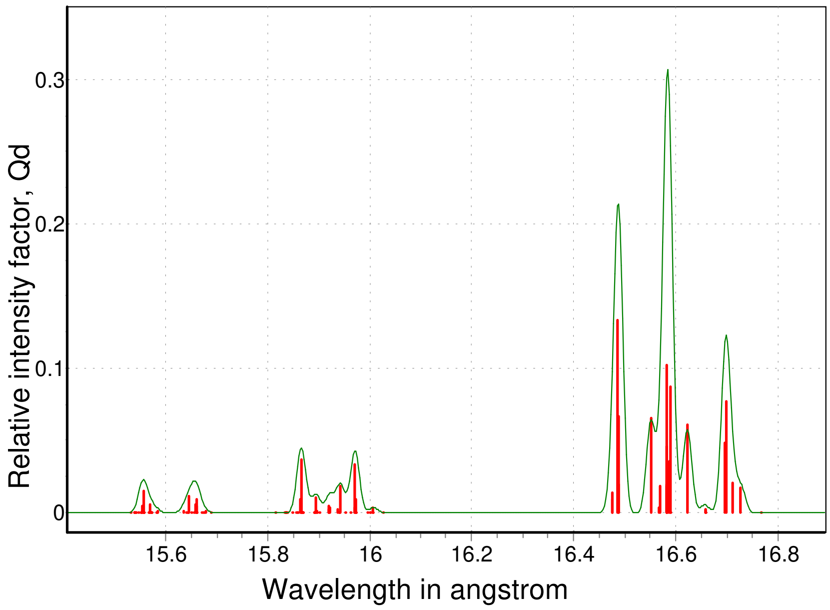

Fig. 12. Dielectronic satellites $2lnl' - 1s2l"$ with n=3-5 in O^{6+}

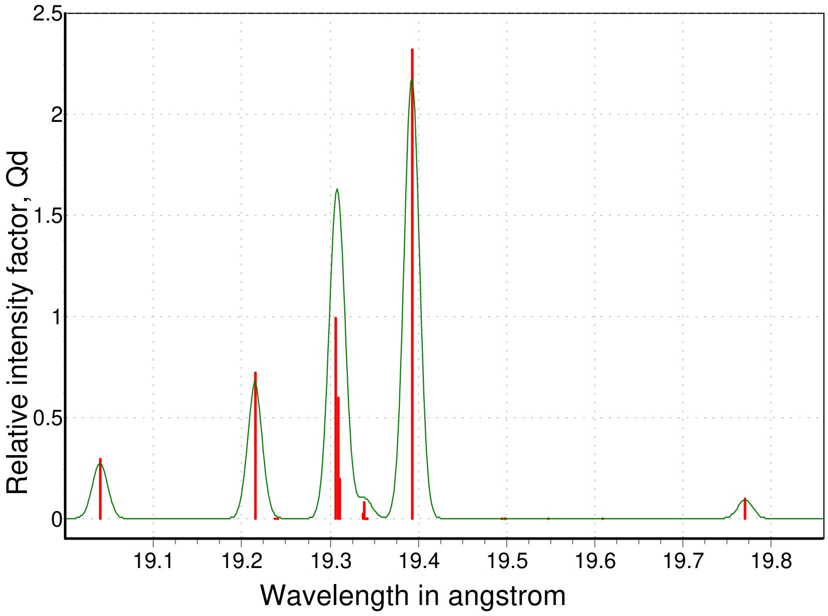

Fig. 13. Dielectronic satellites $2l2l' - 1s2l''$ in O^{6+}

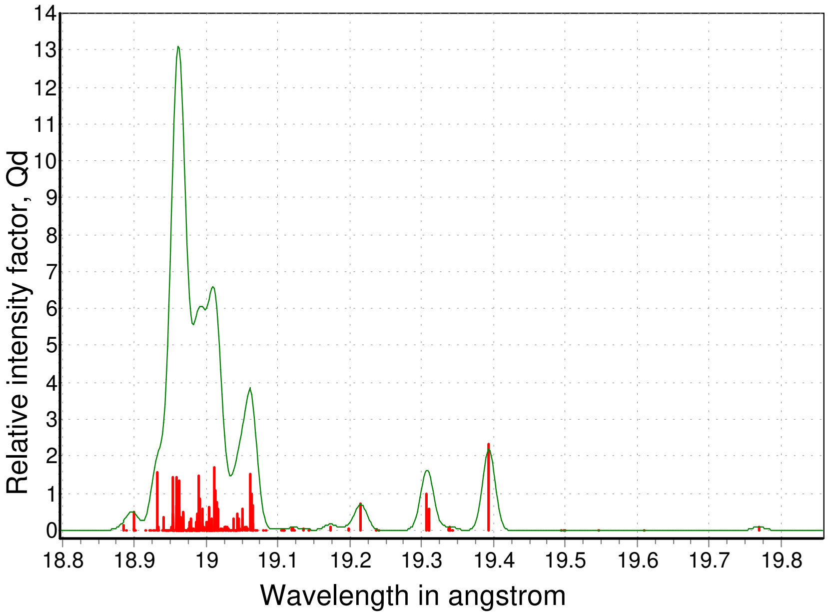

Fig. 14. Dielectronic satellites $2lnl' - 1snl$" with n=2-5 in O^{6+}

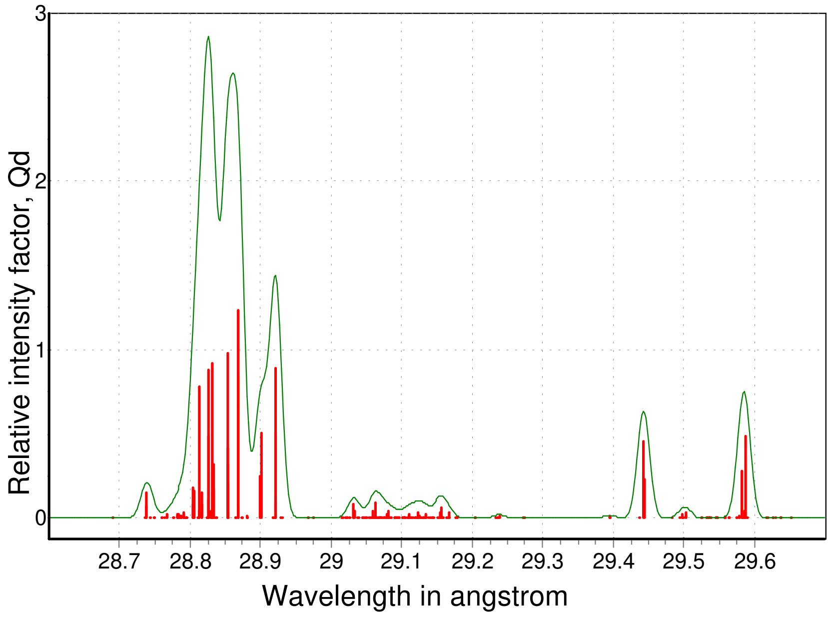

Fig. 15. Dielectronic satellites $1s2lnl' - 1s^2nl$" with n=2-5 in N^{4+}

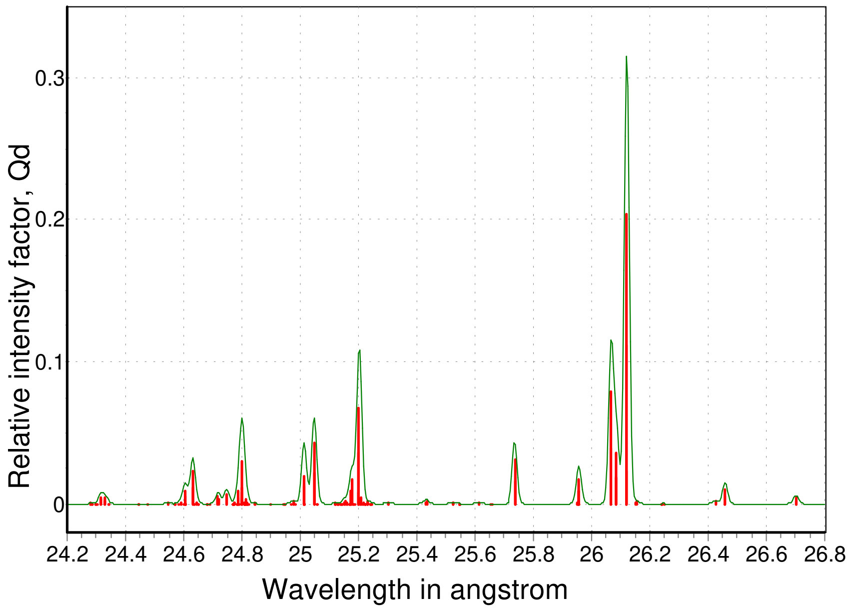

Fig. 16. Dielectronic satellites $1s2lnl' - 1s^22l$" with n=3-5 in N^{4+}

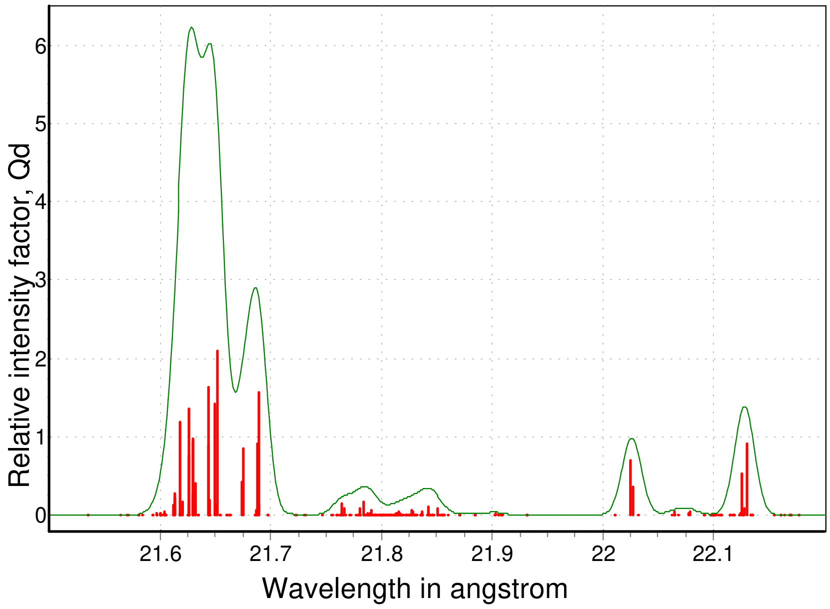

Fig. 17. Dielectronic satellites $1s2lnl' - 1s^2nl$" with n=2-5 in O^{5+}

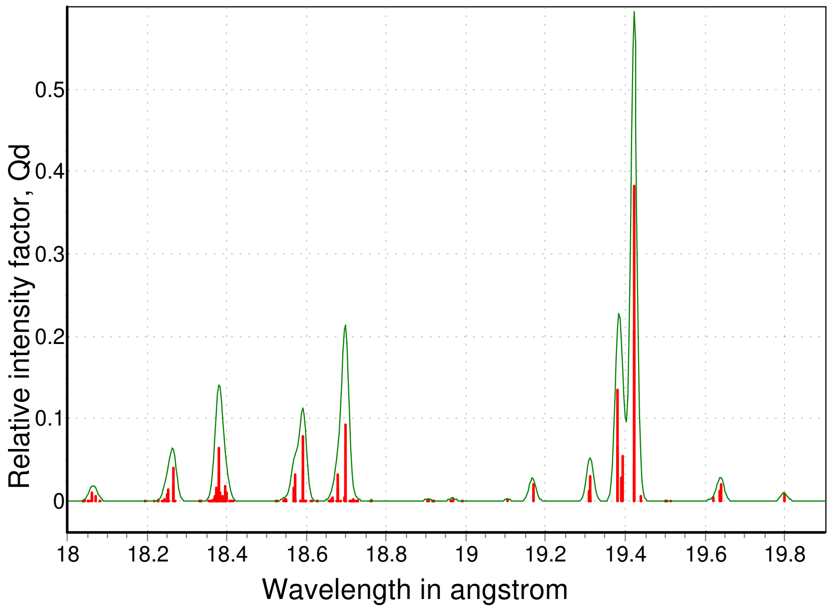

Fig. 18. Dielectronic satellites $1s2lnl' - 1s^22l$" with n=3-5 in O^{5+}